

## METEOSAT BASED AGROMETEOROLOGICAL MONITORING AND CROP YIELD FORECASTING USING THE ENERGY AND WATER BALANCE MONITORING SYSTEM

Andries Rosema, Marjolein de Weirdt, Steven Foppes

Environmental Analysis and Remote Sensing Ltd (EARS)  
Kanaalweg 1, 2628 EB DELFT, Netherlands, ears@ears.nl.

**Commission VIII, WG VIII/10**

**KEYWORDS:** Satellite, Meteosat, MSG, EWBMS, FAST, GMES, GMFS, Geoland, Rainfall, Radiation, Evapotranspiration, Drought, Crop yield, Forecast, Monitoring.

**ABSTRACT:**

This paper provides an overview of the Energy and Water Balance Monitoring System (EWBMS). This Meteosat based system provides continuous agrometeorological data fields over large regions at pixel spatial resolution (3 km) and daily temporal resolution. It is unique in being the first operational source of actual evapotranspiration, which data is the key to soil moisture, crop and pasture growth and regional water balances. In this paper we explain how the EWBMS data products may be used for crop yield forecasting. A dedicated crop yield model (ECGM) has been developed which uses the EWBMS radiation and actual evapotranspiration data to generate estimates of crop production and crop yield forecasts. Some activities carried out in the framework of the GMES projects Geoland and GMFS are introduced. Examples of products and results are shown.

**INTRODUCTION**

The EARS Energy and Water Balance Monitoring System (EWBMS) uses hourly geostationary meteorological satellite data to create daily data field of surface and air temperature, surface albedo, global and net radiation, actual and potential evapotranspiration and precipitation. The system is the first operational source of actual evapotranspiration data. These data are key to the two most important applications of the EWBMS: river basin water management and crop yield forecasting. This paper focusses on agrometeorological data provision and crop yield forecasting in Africa and Europe on the basis of Meteosat Second Generation (MSG) data. We use other geostationary satellites to cover Asia (FengYun-2c, Meteosat 7) and America (GOES).

**SATELLITE DATA PROCESSING**

MSG VIS and TIR data are received hourly with our MSG receiving station in Delft. They are pre-processed automatically to prepare for rainfall and energy balance processing. Clouds are identified, cloud top temperatures are measured and depending on these temperatures cloud heights classes are assigned. For each cloud height class the cloud frequency or “cloud duration” (CD<sub>i</sub>) is count during a day. These cloud durations are input for the rainfall processing.

A second task during pre-processing is to create noon and midnight image composites as input for the energy balance calculations. For mathematical-physical reasons use is made of noon and midnight surface temperatures. However in a noon

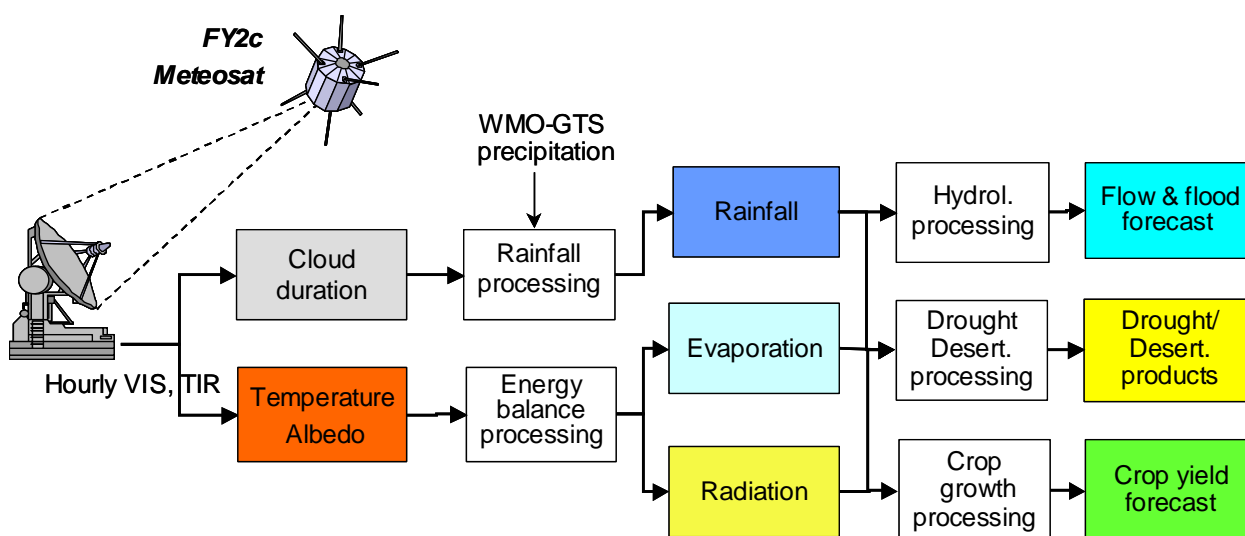


Figure 1: Overview of the Energy and Water Balance Monitoring System

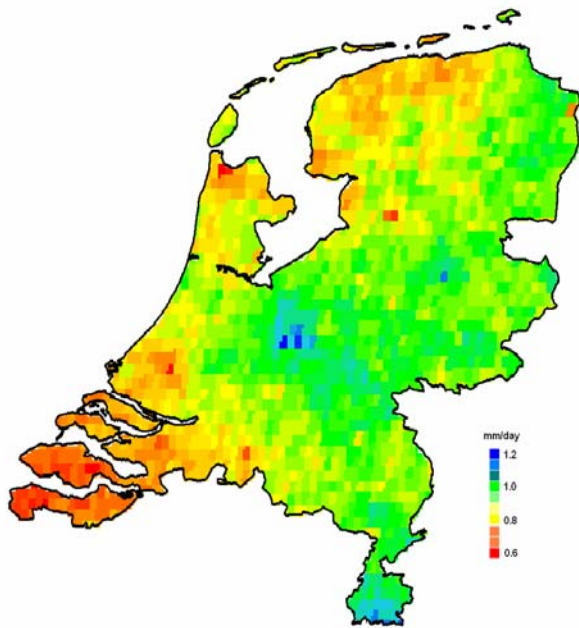


Figure 2: EWBMS average daily rainfall during the period January-April 2006 in the Netherlands, derived from MSG and WMO-GTS data

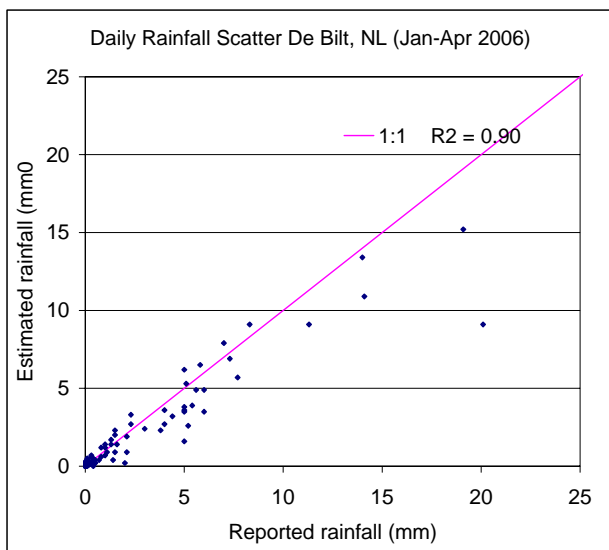


Figure 3: Comparison of predicted and reported daily rainfall as measured at the Royal Netherlands Meteorological Institute in De Bilt, Netherlands.

Meteosat slot the time varies from west to east and is only equal to noon at the centre. For this reason a series of hourly MSG images is used to create composite images where it is (close to) noon or midnight everywhere.

**Rainfall processing**

For the rainfall processing, besides the satellite data, we use WMO-GTS data that are received in near real time via the internet. We describe the relation between the precipitation field and the cloud durations by means of “local regression”. It means that we select a set of 1 central and 11 surrounding rainfall stations. This provides a set of 12 samples of the precipitation field, for which we extract the corresponding

cloud durations. Subsequently a regression equation is calculated which characterizes the relation between rainfall R and cloud durations at the central rainfall station:

$$R = a_0 + a_1.CD_1 + a_2.CD_2 + \dots \quad (1)$$

The coefficients of the regression equation ( $a_0, a_1, \dots$ ) are assigned to the central rainfall station. Then we consider the next rainfall station and the procedure is repeated until for each rainfall station a set of regression coefficients has been determined which characterizes the local rainfall field. Finally each regression coefficient is interpolated by means of inverse distance weighing so as to obtain values of the regression coefficients for each pixel. Hereafter the precipitation in each pixel can be calculated using the regression equation above.

In our rainfall mapping methodology a validation procedure is included. Validation is done by “Jack-knifing”. It means that the whole rainfall mapping is done as many times as there are GTS rainfall stations, but each time leaving another single rainfall station. Each run then provides a single pair of measured and satellite derived rainfall values which are mutually independent. At the end there are as many validation data pairs as there are GTS rainfall stations. The quality of the relation is then determined by calculating the correlation coefficient and standard error of estimate. An example for daily rainfall in the Netherlands is shown in figures 2 and 3.

**Energy balance processing**

Processing for the surface energy balance components is based on physical laws, rather than statistical relations. First calibration equations are applied to convert the thermal infrared and visual digital values to planetary temperature ( $T_0'$ ) and planetary albedo ( $A'$ ), i.e. the temperature and albedo as observed through the atmosphere. We use a “2-flux” atmospheric transmission model to convert the planetary values to values of the surface temperature ( $T_0$ ) and surface albedo ( $A$ ). No information on atmospheric composition is needed. In stead use is made of within image references like lowest albedo and highest surface temperature.

A new methodology has been developed to derive the boundary layer air temperature ( $T_b$ ). The regression between observed noon and midnight surface temperatures in a sub-window usually shows a linear relation:

$$T_{12} = a.T_{24} + b \quad (2)$$

Where regression is not accurate enough, the coefficient a in (2) is derived on the basis of a model of the course of the daily surface temperature. For the case of perfect heat transfer to the atmosphere, the noon and midnight surface temperature would be equal to the boundary layer air temperature, i.e.

$$T_{12} = T_{24} = T_b \quad (3)$$

From (2) and (3) we may solve the boundary layer air temperature  $T_b$ . A boundary layer air temperature map is obtained by shifting the window pixel by pixel across the satellite data fields. By combination of the observed surface temperature  $T_0$  and the boundary layer temperature  $T_b$  we can make an estimate of the air temperature at observation height ( $T_a$ ). Observation height air temperature is a by-product of the EWBMS system that is also used for validation, whereas such air temperatures are also available from GTS reports.

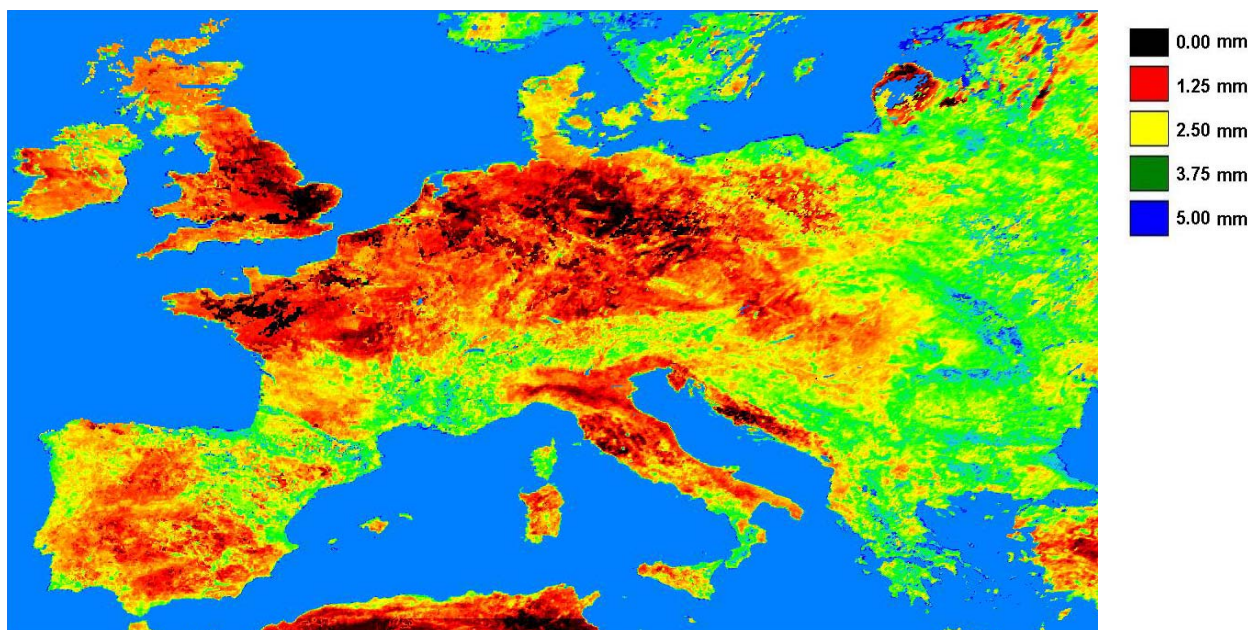


Figure 4: EWBMS actual evaporation during 18-20 July 2006, showing this summer's intense drought in NW Europe

Hereafter we calculate the global radiation at noon. This involves the earlier mentioned 2-flux model of atmospheric transmission to calculate the global radiation at the ground surface. The noon value is then converted to a daily average value of the global radiation ( $I_g$ ) using Fourier analysis of the daily solar cycle. Hereafter the upgoing thermal radiation flux ( $I_u$ ) is estimated from the surface temperature, and the downgoing radiation flux from the boundary layer air temperature ( $I_d$ ). The net radiation ( $I_n$ ) is then obtained with:

$$I_n = (1-A) I_g + I_d - I_u \quad (4)$$

The next step of the energy balance processing is the calculation of the sensible heat flux into the atmosphere ( $H$ ) with:

$$H = \alpha (T_0 - T_b) \quad (5)$$

Where  $\alpha$  is the atmospheric heat transfer coefficient. Having determined the daily average values of the net radiation  $I_n$  and the sensible heat flux  $H$ , we can find the latent energy  $LE$ , i.e. the energy used for evaporating water, from

$$LE = I_n - H \quad (6)$$

Our research has shown that for vegetation it is necessary to involve an additional term in the energy balance, which represents the energy used for photosynthetic electron transport. The value is in the order of 5-10% of the global radiation. From the latent energy flux  $LE$  (in  $W/m^2$ ) we can determine the actual evaporation ( $E$ ) in mm/day. About  $28 W/m^2$  is required for evaporating 1 mm of water. An actual evapotranspiration map for Europe, July 2006, is shown in figure 4. This map clearly depicts this summer's drought in NW Europe.

If sufficient water is available the evaporation is potential ( $LE_p$ ). By means of the Penman-Monteith equation it can be shown that:

$$LE_p \approx 0.8 I_n \quad (7)$$

The relative evapotranspiration (RE) is then defined as

$$RE = LE / LE_p \quad (8)$$

The relative evapotranspiration is also a product of the EWBMS. It is an important agricultural drought indicator (because it is radiation independent) and, as we will see, is directly related to crop growth. It represents actual crop water use and therefore is a better indicator of crop growth than rainfall.

### CROP GROWTH SIMULATION

The EWBMS data fields of rainfall, actual evapotranspiration and radiation may be used for crop yield forecasting in several ways. The most direct approach would be to use the accumulated rainfall or actual evapotranspiration during the crop growing period as crop growth indicator and then to establish an empirical relation between such indicators and reported crop yields. A multi year data set will be required. The required satellite data are available, as we are receiving and archiving Meteosat data since 1993.

A more sophisticated approach to crop yield is the use of deterministic crop growth models. Many crop growth models use rainfall data as input, because in the past only such data were available. A source of inaccuracy in this approach is the estimation of amount of water available to the crop. This involves a number of assumptions in relation to rainfall runoff and rainfall storage in the soil. Crude simplifications of unsaturated zone soil moisture storage and transport are made.

In Africa rainfall measurements are scarce and in some areas not available at all. Nowadays some use is made of distributed rainfall data generated by weather prediction models. However rainfall prediction is usually the weakest part of such models. Actual rainfall fields are usually dislocated relative to their forecast. A much better source of data for crop yield estimation is available from the EWBMS system.

The EWBMS provides continent wide data fields of actual evapotranspiration at daily temporal and 3 km spatial resolution. It is well established that actual evapotranspiration closely represents the actual water use by plants (*Doorenbos and Kassam 1979*). Although Meteosat cannot resolve each individual field, it has been shown that Meteosat derived actual evapotranspiration is very useful for estimation crop growth and forecasting yield. The evapotranspiration data avoid the inaccurate soil moisture budget component in classical rainfed crop growth models. Moreover the evapotranspiration data are available for each 3\*3 km pixel of Africa and Europe in near real time.

### EARS Crop Growth Model (ECGM)

In this section we explain how a simple dedicated crop growth model may be developed and used, which is fed by the EWBMS actual evapotranspiration and radiation data. This model is based on three main principles:

- (1) Crop growth depends mainly on radiation interception and hardly on species (*Monteith 1977*),
- (2) Crop growth is proportional the actual evapotranspiration (*Stewart 1973, Doorenbos & Kassam 1979*),
- (3) Crop growth is CO<sub>2</sub> limited, which leads to a radiation use efficiency, which decreases hyperbolically with increasing radiation (*Rosema et al. 1998*)

In the ECGM the daily gross photosynthesis (P) is calculated with:

$$P = c \cdot \varepsilon \cdot C \cdot RP \cdot I_g \quad (9)$$

Where “c” is a conversion factor,  $\varepsilon$  is the photosynthetic efficiency of radiation, C is the crop coverage, RP the relative production and  $I_g$  the global radiation. In the above expression the crop coverage is estimated from the crop biomass with:

$$C = B/B_c \quad (C=1 \text{ for } B \geq B_c) \quad (10)$$

Here  $B_c$  is the biomass at crop closure. This equation corresponds to exponential initial growth. The calculation of the relative production as a result of water limitation is based on the well-known relation developed by *Stewart (1973)* and extensively documented in *Doorenbos & Kassam (1979)*:

$$RP = 1 - k_y(1 - RE) \quad (11)$$

The yield respons factor  $k_y$  depends on the drought resistivity of the crop and is for example 1.25 for maize, 1.0 for winter wheat and 0.8 for sorghum and millet.

The formulation of the photosynthetic efficiency results from our research on the relation between chlorophyll fluorescence and photosynthetic electron transport. Equilibrium between photosystem reaction centre charging and drainage leads to the following relation

$$\varepsilon = 1/(1.25 + r_e \cdot I_g) \quad (12)$$

where  $r_e$  is a the resistance for electron transport (~0.01). We have discussed the factors determining gross photosynthesis rate. The main quantities determining this rate are the global radiation  $I_g$  and the relative evapotranspiration RE. These data can be obtained from the EWBMS system.

A part of the sugar stored as a result of the photosynthesis process is burned again to provide energy for crop biomass maintenance. This maintenance respiration (Re) is calculated on the basis of the relation provided by Supit (1994)

$$Re = c_r \cdot B \cdot q_{10}^{(T-T_{ref})/10} \quad (13)$$

For our purpose this relation has been adapted as follows

$$Re = c_r \cdot B \cdot q^{RE} \quad (14)$$

Now the net daily biomass production is given by

$$\Delta B = P - Re \quad (15)$$

Using the daily EWBMS radiation and relative evapotranspiration products as input we may now accumulate the biomass during the growing season on a day-by-day basis.

$$B_{i+1} = B_i + \Delta B \quad (16)$$

The ECGM software requires the specification of the start of the growing season. This may be done in several ways: fixed date, starting dekad map, or an automatic start. The automatic start requires that the relative evapotranspiration exceeds a specified treshold ( $RE > RE_c$ ). We can also run the crop growth model for non water limited conditions, i.e. for  $RE = RP = 1$ . This leads to the potential biomass  $B_p$ . We define the relative biomass at any moment of the growing season (RB) as the ratio of the actual over the potential biomass:

$$RB = B / B_p \quad (17)$$

### CROP YIELD FORECASTING

The absolute value of the biomass simulated with a crop growth model is usually not very accurate. The reason is that models are relatively simpel, or, when they are more complex, require too much input data, which data is not available across large areas. For this reason we follow a “relative” approach to crop yield forecasting, which makes use of more yearly satellite derived and reported yield. The following approach is often used. It is first assumed that the economic yield is proportional to the crop biomass and that consequently the relative biomass equals the relative yield:  $RY = RB$ . We determine from 5 years of satellite data the average relative biomass:

$$RB^{\oplus} = \sum RB_i / 5 \approx \sum (B_i) / (5 \cdot B_p) \quad (18)$$

The current years relative biomass as derived from the satellite is given by (17). We now define the difference biomass as the fractional difference of the current year simulated biomass relative to the average biomass of the previous 5 years:

$$DB = RB/RB^{\oplus} - 1 \quad (19)$$

Assuming that we have the observed yields of the previous five year available, we can calculate the average observed yield  $Y^{\oplus}$ . Rather than the absolute biomass B, the ECGM produces the relative biomass RB and the difference biomass DB as standard products because they are more accurate than the absolute biomass B. From the DB product we may obtain the crop yield forecast (Y) with:

$$Y = (DB+1) \cdot Y^{\oplus} \quad (20)$$

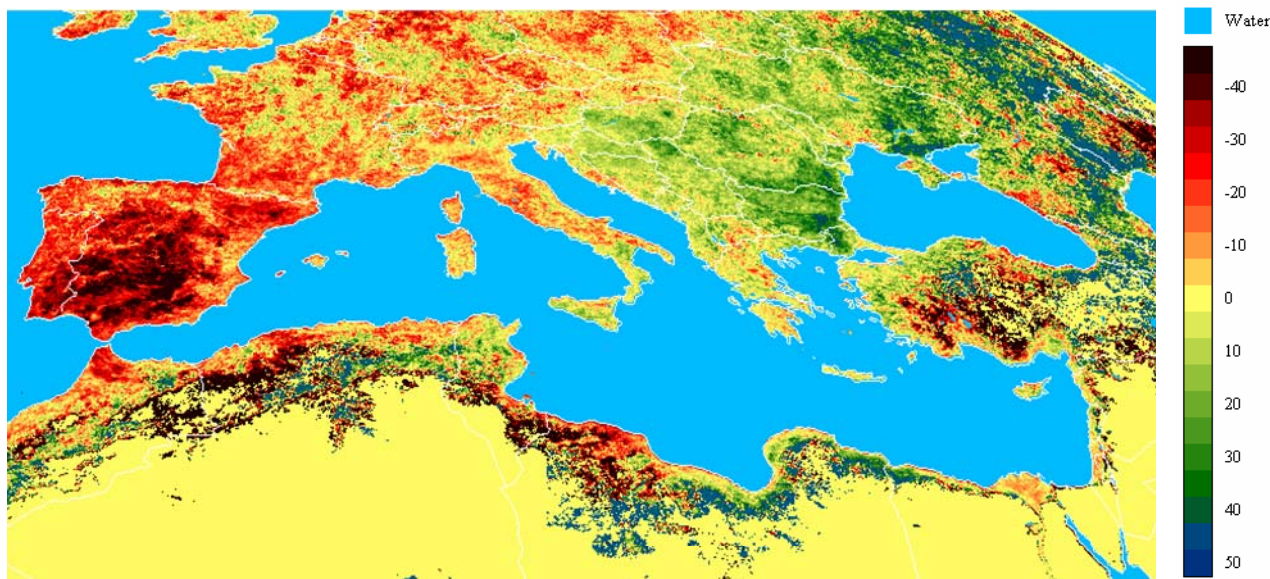


Figure 5: EWBMS difference biomass for wheat in the Euromed region, August 2005. The deviation from average (yellow) is quantified by the scale on the right. Western Europe and particularly Portugal and Spain had an unfavorable growing season (red, black). The Balkan countries and Oekraine show above average yield expectation (green)

Country	Difference from avrg(%)	Forecasted Wheat yield (Hg/Ha)
Albania	5	31302
Austria	-3	48462
Belarus	3	26425
Belgium	-13	72736
Bosnia Herzeg.	8	31589
Bulgaria	24	37337
Croatia	7	41730
Cyprus	0	20180
Czech Rep.	-7	43760
France	-10	63024
Germany	-7	68322
Greece	1	23684
Hungary	10	42259
Italy	-4	29947
Macedonia	-2	25400
Moldavia	11	22666
Netherlands	-9	77521
Poland	-6	33697
Portugal	-29	9249
Rumania	17	29434
Serbia Mont.	13	34644
Slovakia	0	38018
Spain	-32	19549
Switzerland	-5	54459
Turkey	-6	20094
Ukraine	15	29327
United Kingdom	-2	75968

Table 1: Wheat yield forecast European countries Sept. 2005

It is noted that the difference biomass DB may be determined at any moment during the growing season from the simulated actual and potential biomass according to (19). It also means that we can make a crop yield forecast with (20) at any moment of the growing season. It has been shown that a reliable yield forecast is possible from about 70 days after planting/sowing. As we usually have to produce crop yield forecasts for administrative units (for which we have historic yield data) the procedure is usually such that we use the EWBMS and ECGM to generate RB and DB image products. Hereafter we spatially average the results for the crop growing area within the specific administrative unit. Finally we calculate the forecasted yield with (20). The better the crop mask that is used, the better the results will be.

Another approach to crop yield forecasting, as usually followed at JRC, makes use of regression between the observed yields (Y) and satellite derived yield indicators (I). Based on the historic data a regression equation is determined:

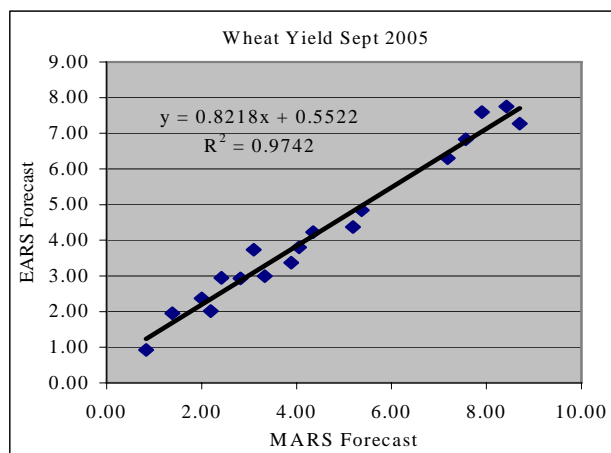


Figure 6: Comparison of EARS and MARS yield forecast in 2005 (courtesy Jacques Delincé, JRC Agrifish unit)

$$Y = a_0 + a_1.I_1 + a_2.I_2 + a_3.I_3 + \dots \quad (21)$$

Yield indicators from the EWBMS system can be: the rainfall (R), the actual or relative evapotranspiration (E, RE), and the simulated or relative biomass (B, RB). All these indicators are accumulated or simulated up to the current moment of the growing season and are spatially averaged for the relevant crop growing areas and administrative units. Once a regression equation has been determined for each administrative unit, this equation may be used for yield forecasting in the next year.

### Geoland project

In the framework of the Geoland-OFM project we have prepared maize and wheat yield indicators for Spain, Belgium and Poland at the level of NUTS-2 administrative units. Similar yield indicators have been generated for a large number of counties in the provinces Hebei, Shanxi, Henan, Shandong, Beijing and Tianjin in China, using data from the Japanese GMS satellite of the years 1999-2001. All indicators have been provided to OFM coordinator Alterra. Results have been analyzed in detail by the AGRIFISH unit of the EU Joint Research Centre in Ispra (Genovese, Bettio and Fritz, 2006) following the regression approach of equation (17). Results may be discussed in other presentations at this conference.

In addition to the previous activities we have carried out a crop yield forecast for a large number of European countries (NUTS-1 level) at the end of August 2005. See figures 5, 6 and table 1 on the previous page. This forecast was compared by the JRC-Agrifish unit with their own forecast based on weather data and the CGMS model. The results for wheat and barley were very much the same ( $r^2 \approx 0.95$ , see figure 6).

### GMFS project

In the framework of the GMES project Global Monitoring for Food Security we have produced operational crop yield forecasts for Africa. These "FAST" activities (*Food Assessment by Satellite Technology*) consisted of (i) providing timely EWBMS crop growth and yield forecast data fields to partners and users by ftp, and (ii) preparing region and country specific crop yield forecasting bulletins in support of FAO/WFP Crop and Food Supply Assessment Missions. Such missions are usually undertaken on request of countries, which have an emerging food production problem and want to apply for food aid. We have produced 24 regional and national crop yield forecast bulletins. The FAST bulletins were their earliest source of quantitative crop yield information.

### Concluding remarks

The EWBMS system is an abundant source of agrometeorological information relevant for crop yield forecasting. The data products have some explicit advantages. They are: quantitative, continuous in space and time, synoptic, uniform, objective, validated and economic. In the framework of the Geoland and GMFS projects we have demonstrated being able to make reliable and timely crop yield forecasts for every province in Europe and Africa from halfway the growing season. The economic aspect should not be neglected. The system is based on low cost satellite receiving and processing technology. Generating a crop yield forecast for most European countries and creating and distributing the corresponding early warning bulletin took 5 person days.

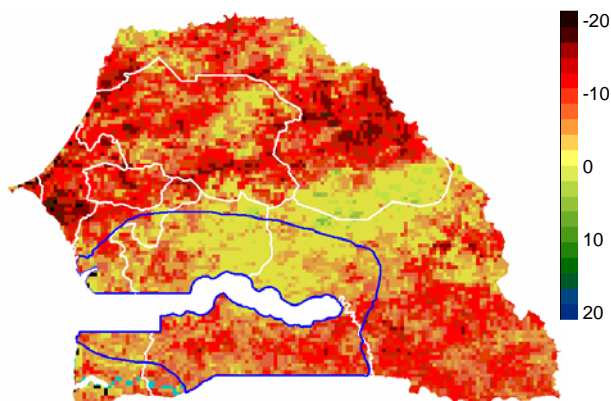


Figure 7: Sorghum difference yield (%), Senegal 2004, GMFS

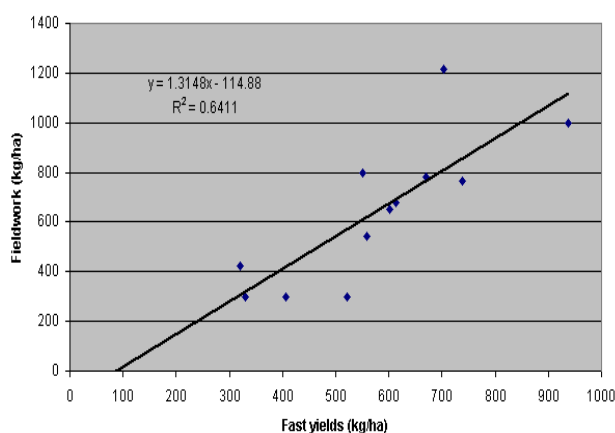


Figure 8: Validation of FAST yields by fieldwork in GMFS. (Courtesy Synoptics, Wageningen)

### REFERENCES

- Doorenbos and Kassam (1979) Yield response to water, *FAO Irrigation and Drainage Paper 33*, FAO Rome.
- Monteith (1977) Climate and efficiency of crop production in Britain, *Philos. Trans. R. Soc.*, London, Series B, 281: 277-294.
- Rosema et al. (1998) The relation between Laser-Induced chlorophyll fluorescence and photosynthesis, *Remote Sensing of Environment*, 65, p. 143-153.
- Stewart and Hagan (1973) Functions to predict effects of crop water deficits, *ASCE J. Irrig. and Drainage Div.* 99, p. 421-439.
- Supit et al (1994) System description of the WOFOST 6.0 crop simulation model implemented in CGMS. *Publ. of the EC EUR 15956*, Luxembourg. 1994-146 p. cat.no: CL-NA-15956-EN.
- C.Genovese, Bettio and Fritz (2006) Report on Yield Intercomparison study, *Geoland project report*, JRC-IPSC, Agrifish Unit, Ispra.